Journal of Power Sources 392 (2018) 274–284

Contents lists available at ScienceDirect

Journal of Power Sources

journal homepage: www.elsevier.com/locate/jpowsour

A comparison of rotating disc electrode, floating electrode technique and membrane electrode assembly measurements for catalyst testing

Sladjana Martens[a], Ludwig Asen[a,b], Giorgio Ercolano[c], Fabio Dionigi[d], Chris Zalitis[e], Alex Hawkins[e], Alejandro Martinez Bonastre[e], Lukas Seidl[a,f], Alois C. Knoll[a], Jonathan Sharman[e], Peter Strasser[d], Deborah Jones[c], Oliver Schneider[a,*]

[a] Institute for Informatics VI, Technical University of Munich, Schleißheimerstr. 90a, D-85748 Garching, Germany
[b] Department of Chemistry, Technical University of Munich, Lichtenbergstraße 4, D-85748 Garching, Germany
[c] Institut Charles Gerhardt Montpellier, UMR 5253 CNRS-UM-ENSCM, Université de Montpellier, Place E. Bataillon, Bât 15, cc 1502, 34095 Montpellier Cedex 5, France
[d] The Electrochemical Catalysis, Energy, and Material Science Group, Department of Chemical Engineering, Technische Universität Berlin, Straße des 17. Juni 124, 10623 Berlin, Germany
[e] Johnson Matthey Technology Centre, Blount's Court, Sonning Common, Reading, RG4 9NH, UK
[f] Physics Department, Technical University of Munich, James-Franck-Str. 1, D-85748 Garching, Germany

HIGHLIGHTS

- Reliable results obtained by new rotating disc electrode catalyst testing protocol.
- RDE data comparable to MEA and floating electrode technique (FET) measurements.
- FET unifies advantages of RDE and MEA.
- FET permits measurements with low amounts of catalyst at high currents.
- New degradation testing protocol results in similar changes in RDE, FET and MEA.

GRAPHICAL ABSTRACT

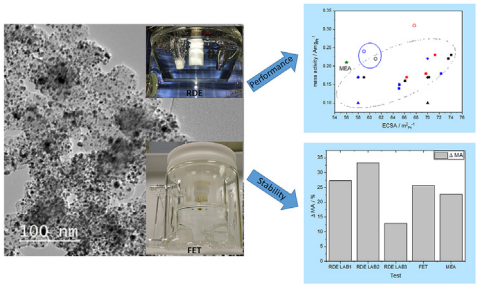

ARTICLE INFO

Keywords:
Hydrogen fuel cell
Rotating disc electrode
Floating electrode technique
Membrane electrode assembly
Testing protocol

ABSTRACT

The development of new catalysts for low temperature fuel cells requires accurate characterization techniques to evaluate their performance. As initially only small amounts of catalyst are available, preliminary screening must rely on suitable test methods. In this work, using a carbon supported platinum benchmark catalyst, the rotating disc electrode (RDE) technique was revisited in order to develop a detailed testing protocol leading to comparable results between different laboratories. The RDE results were validated by comparison with data measured both in proton exchange membrane single cells and via the relatively new floating electrode technique. This method can be operated with small amounts of catalyst but does not suffer from low limiting currents and allows prediction of high current capability of newly developed catalysts. Different durability testing protocols were tested with all three methods. Such protocols need to be able to introduce changes in the reference catalyst, but must not be too harsh as otherwise they cannot be applied to alloy catalysts. In all protocols an upper

* Corresponding author.
E-mail addresses: sladjana.martens@tum.de (S. Martens), ludwig.asen@tum.de (L. Asen), giorgio.ercolano@umontpellier.fr (G. Ercolano), fabio.dionigi@tu-berlin.de (F. Dionigi), Chris.Zalitis@matthey.com (C. Zalitis), alex.hawkins@matthey.com (A. Hawkins), Alex.Martinez.Bonastre@matthey.com (A. Martinez Bonastre), lukas.seidl@tum.de (L. Seidl), knoll@in.tum.de (A.C. Knoll), jonathan.sharman@matthey.com (J. Sharman), pstrasser@tu-berlin.de (P. Strasser), deborah.jones@umontpellier.fr (D. Jones), oliver_m.schneider@tum.de (O. Schneider).

https://doi.org/10.1016/j.jpowsour.2018.04.084
Received 17 January 2018; Received in revised form 19 April 2018; Accepted 24 April 2018

potential limit of 0.925 V was used, as this produced degradation in the chosen benchmark catalyst, but still represents realistic conditions for alloy catalysts.

1. Introduction

The transportation sector caused nearly 20.5% of total CO_2 emissions in 2014 [1]. This is one reason for the increased interest in electrically driven vehicles (EVs) [2]. The batteries used in battery EVs suffer from low energy density, limited driving range and long charging times [2,3]. Fuel cells (FCs) provide a large driving range of ~500 km, but suffer from high cost due to high Pt content and limited lifetime [4]. Currently, both cathode and anode sides of FCs contain Pt-based catalysts supported on carbon (Pt/C) [5]. While the kinetics of the hydrogen oxidation reaction (HOR) at the anode is very fast, the oxygen reduction reaction (ORR) at the cathode side has a sluggish kinetics, causing voltage losses of hundreds of millivolts [6–8]. Furthermore, Pt catalysts can suffer from poisoning by impurities in fuels, dissolution and agglomeration of Pt particles [9–11]. Costs of the FCs can be reduced by using Pt alloys with increased ORR activity or by complete replacement of Pt [12–14].

Developing new cathode catalysts requires reliable methods to evaluate activity and stability. The data most representative for actual FC performance are obtained by measurements on membrane electrode assemblies (MEA). However, MEA fabrication and characterization are time-consuming, require specific instrumentation, accurate control of gas pressures, temperatures and relative humidities, and large amounts of catalyst material. Newly synthesized catalysts are prepared first in small amounts [15]. Therefore, half-cell tests in aqueous perchloric acid electrolytes ($HClO_4$) are preferred for initial screening, typically based on hydrodynamic techniques like the channel flow dual electrode [16] and rotating disc electrode techniques (RDE) [17,18], accelerating oxygen access to the surface and assuring constant limiting currents at large overpotentials. For RDE, a catalyst layer is deposited onto the surface of a glassy carbon (GC) electrode embedded in the RDE holder [19–21]. The large current densities common in FC operation cannot be reached because oxygen solubility in $HClO_4$ is low, and limiting currents are small, ~6 mA cm^{-2} at a rotation rate of 1600 rpm. The technique therefore aims at determining the kinetic current at 0.9 V vs. reversible hydrogen electrode (RHE), calculated from the measured current after applying corrections for ohmic potential drop (iR), capacitive background currents, and mass transport (Koutecký-Levich equation) [22,23]. This current is normalized to the total true electrochemical catalyst surface area (ECSA), determined electrochemically (surface specific activity (SA)) or to the total Pt mass on the electrode (mass activity (MA)).

Because of the wide spread of published values for SA and MA even for identical catalysts, several recent papers have revisited the RDE testing procedure. Garsany et al. recommended procedures resulting in reliable ORR benchmarking results [24], and a method for reproducibly producing smooth electrocatalyst thin films [25] by drop-casting the ink followed by rotational drying at 700 rpm. Uniform catalyst layers with negligible difference in ECSA, but exhibiting higher and more reproducible MA were obtained. Shinozaki et al. [15] found highest activities when omitting Nafion from the ink, but adding a non-ionic surfactant, and evaporating the solvent slowly at 40 °C. The use of a freshly prepared RHE reference electrode (RE) and ultrapure chemicals is recommended [26]. $HClO_4$ is the recommended electrolyte due to weak ClO_4^- adsorption, with the concentration determined by a compromise between conductivity and a low impurity level [27]. The determination of the ECSA by hydrogen underpotential deposition (H_{UPD}) results in lower values than by carbon monoxide (CO) stripping [28], explained by a potential-dependent contribution of the support capacitance.

ORR activity is usually measured by linear sweep voltammetry (LSV) from more negative to more positive potentials in order to start with an oxide free Pt surface. Scan rates $\leq 20\ mV\ s^{-1}$ were recommended to minimise capacitive currents [19,29]. At $5\ mV\ s^{-1}$, lower activities were observed, explained by a larger amount of OH_{ads} on the surface and stronger impurity adsorption [19,24,29].

In the new floating electrode technique (FET) developed by Zalitis et al. [30] the ink is applied onto a porous Au coated polycarbonate membrane floating on the electrolyte. Oxygen can reach the catalyst directly through the membrane pores from the gas phase, enhancing mass transport by several orders of magnitude compared to RDE. MA at 0.9 V can be determined without mass transport correction.

The present study is based on the benchmarking of a Pt/C catalyst at four research sites (Lab1–Lab4) with RDE, FET and MEA measurements. After applying current recommendations and protocols, discrepancy was found between the RDE results at Lab1 - Lab3 leading us to further elaborate the procedures and to compare the SA, MA and ECSA obtained with those derived from FET and MEA results (Lab4). Even though no full quantitative agreement can be expected, the general trends in activity and durability must be reflected correctly and be representative for the behavior in an MEA. The results must not depend on the laboratory where they are obtained. Protocols need to be universal enough to be applicable to alloys and pure Pt/C. For this work, a Pt/C catalyst from JMFC was selected as benchmark catalyst. Based on prior experience and the literature, experiments were carried out to optimize certain experimental parameters. Thereby a detailed RDE measurement protocol was established and applied, leading to results reproducible and comparable between groups, and in reasonable agreement with FET and MEA experiments.

2. Experimental

2.1. Catalysts, chemicals and gases

The 50 wt% Pt/C catalyst (JMFC) was characterized by transmission electron microscopy (TEM) and energy dispersive X-ray spectroscopy (EDS). Isopropanol (IP, Sigma Aldrich, anhydrous 99.5%), 5 wt% Nafion (Sigma Aldrich, Nafion 1100 EW) and 18.2 $M\Omega\ cm^{-1}$ water were used to freshly prepare a catalyst ink (concentration: 0.2 mg_{Pt} ml^{-1}) by adding 4 mg of 50 wt% Pt/C catalyst to a mixture of 7.96 ml water, 2 ml IP and 40 µl 5 wt% Nafion solution and ultrasonicating it for 15 min to disperse the catalyst homogeneously. Prior to use, it was sonicated for additional 40 s. For the sonication a Bandelin Sonopulse HD 3200, a Branson Sonifier 150 or a Branson Digital Sonifier 450, all with a 3 mm outer diameter horn tip were used at the lowest possible intensity. To limit ink warming, the container was placed in a water or ice bath during sonication. 10–30 µl ink were applied to the electrode (catalyst loading of 10–30 $\mu g_{Pt}\ cm^{-2}$). Electrochemical measurements were carried out in freshly prepared 0.1M $HClO_4$ (from concentrated $HClO_4$, Acros Organics, p.A., Fluka TRACEselect, Ultrex II Ultrapure Reagent (JT Baker) or Sigma Aldrich). Gases for purging of cells and electrolyte were Ar (5.0, Westfalengas), N_2 (Air Liquide Ultrapure) and O_2 (5.0, Westfalengas or Air Liquide Ultrapure).

2.2. Electrode preparation

The GC electrode (ø 5 mm) was polished to a mirror finish using 1 µm alumina-particle suspension (MicroPolish™Buehler) on a moistened polishing microcloth (Buehler MicroCloth PSA) and then 0.05 µm alumina-particle suspension (MicroPolish™Buehler) on a nylon

polishing cloth (Buehler Minimet). Afterwards, the electrode was thoroughly rinsed with water, then ultrasonicated first in water, then in isopropanol and again in water, each for 4 min. In between, the electrode was rinsed with water. After final rinse with water it was dried under N_2 flow. The clean electrode was mounted onto the RDE shaft and – for a loading of 20 μg_{Pt} cm^{-2} – a 20 µl ink droplet was placed onto it (usually two 10 µl aliquots). Stationary drying in air led to inhomogeneous layers. By drying under rotation (700 rpm), it was possible to obtain a homogeneously dispersed catalyst ink covering the GC completely and not covering any of the Teflon. Alternative ways for drying of the ink were use of a 60 W lamp/heater or an oven at 60 °C.

2.3. Electrochemical setup

Electrochemical glass cells suitable for working in controlled atmospheres, in part with a cooling jacket, were thoroughly cleaned, *e.g.* sequentially in a KOH/IP bath, boiling water, immersion in Caro's acid (H_2SO_4/H_2O_2 = 1:1) bath for 6 h or more, thorough rinsing and boiling in water, or a cleaning procedure based on a mix of H_2SO_4 (98%) and Nochromix (an oxidizer), followed by cleaning in nitric acid or a procedure with sulfuric acid and once a month with a permanganate bath. Either an in-house fabricated RHE [31] or a Mercury/Mercurous Sulfate electrode (MMS) (calibrated vs. an RHE) were used as RE. All potentials in this paper are referred to RHE. A Pt wire or a carbon rod (MaTecK, MC002) served as the counter electrode (CE). Electrochemical measurements were carried out with standard laboratory potentiostats (Ivium Compactstat Plus, Biologic SP-300). The catalyst coated RDE working electrode (WE) was controlled by Pine instruments setups.

2.4. RDE measurements

For establishing the RDE protocol, the influence of catalyst loading (10–30 μg_{Pt} cm^{-2}), catalyst layer quality, conditioning upper potential, LSV scan rate for ECSA determination and ORR evaluation, and $HClO_4$ purity on ECSA and MA of the catalysts was evaluated. In addition, a stability testing protocol was established. The protocol then was used for measurements in all the labs.

After assembling and filling the cell with 0.1 M $HClO_4$, inert gas was purged through and above the electrolyte for ~30 min. The electrode was immersed under rotation at 1600 rpm and potential control at 0.05 V, to avoid undefined open circuit exposure. Also between the experiments, the electrode was always potential-controlled or withdrawn from solution. The rotation was then stopped. During experiments, inert gas was purged above the electrolyte. All experiments were carried out in Ar or N_2 atmosphere, if not stated differently.

2.4.1. Conditioning and ECSA determination

For conditioning/cleaning of the Pt/C coated electrode, 100 potential cycles (or as many as needed to obtain a stable voltammogram) at 100 mV s^{-1} were recorded between 0.05 and 1.0 V (or 1.2 V). For ECSA determination, the potential was cycled between 0.05 and 1.0 V at 20 mV s^{-1} (100 mV s^{-1}) for 3 cycles. The H_{UPD} charge was determined by integrating the current in the negative going sweep of the last scan between an upper potential limit where the cathodic current corresponds to the capacitive background current (normally ~0.4 V) and a lower potential limit, taken as the potential of "minimum current" before onset of the hydrogen evolution reaction (HER) (normally ~ +0.05 V), assuming a value [15] of 210 µC cm^{-2} for adsorption of a hydrogen monolayer, after subtraction of the capacitive background current.

$$ECSA = \frac{\frac{1}{v}\cdot\int_{0.4V}^{0.05V}[I - I(0.4V)]dE}{2.1\cdot10^{-4}C\cdot cm_{Pt}^{-2}} \quad (1)$$

2.4.2. Electrochemical impedance spectroscopy (EIS) measurement

A potential of 0.5 V was applied for 1 min, followed by an impedance measurement from 100,000 Hz to 10 Hz at an AC amplitude of 10 mV. The electrolyte resistance was determined by extrapolation of the linear part of the plot Im (Z) vs. Re (Z) to Im (Z) = 0.

2.4.3. ORR testing

For background correction, measurements at 1600 rpm were first carried out in inert gas atmosphere. A potential of 0.05 V was applied for at least 30 s. Thereafter, LSV was measured between 0.05 and 1.0 V at 20 mV s^{-1} (5 mV s^{-1}) and repeated twice. The electrode was then raised above the electrolyte to prevent readsorption of potentially present impurities. After purging of pure oxygen through the electrolyte for at least 30 min, the electrode was reinserted under an applied potential of 0.05 V, and another three LSV measurements were conducted. In the case of a noticeable decrease in diffusion limited currents, oxygen was bubbled in between the scans.

2.4.4. Stability test

The final step of the measurement protocol is a stability test. Different atmospheres (oxygen, inert gas) and lower potential limits were tested. iR compensation during the measurements was applied to avoid potential deviations especially in oxygen atmosphere. Finally, stability evaluation was performed in inert gas atmosphere (electrode raised above solution, 35 min inert gas purging, reimmersion at a potential of 0.925 V). The electrode was then cycled between 0.925 V and 0.6 V at 100 mV s^{-1} for totally 10,000 cycles under constant inert gas purging above the electrolyte. The conditioning step and ORR measurement at 1600 rpm were then repeated and the activities of the catalysts before and after the stability test evaluated and compared.

2.5. Fuel cell testing

The MEAs used in this work consist of five layers. Nafion 1100 EW (equivalent weight, g polymer/mol H^+) was used to fabricate thin-layer electrodes. The cathode catalyst layers had an ionomer/carbon weight ratio of ca. 0.8/1 and metal loadings of ca 0.2 mg_{Pt} cm^{-2}, unless specified otherwise. The anode catalyst layer was kept constant at an ionomer/carbon weight ratio of ca. 1.5/1 and a metal loading of 0.1 mg_{Pt} cm^{-2}. The membrane used was a perfluorosulfonic acid type (JMFC, ~20 µm thick). Catalyst layers were produced on a PTFE substrate and transferred via a decal method onto the membrane. After fabrication of 50 cm^2 MEAs, the active area on each electrode was reduced to 6 cm^2, (3 × 2) cm, with the lamination of a seal over the electrode area. Commercially available gas-diffusion layers (GDLs), based on teflonated carbon fibre paper substrates, were used and adjusted to optimize gas and water transport at the electrodes. Single cells (50 or 6 cm^2 active area) were assembled by sandwiching the catalyst coated membranes between the GDLs and applying an average compression onto the active area.

The fuel cell station was built in-house at JMFC. Pure oxygen and synthetic air were used as cathode reactants and pure H_2 as the anode reactant (all gases of 99.9% purity). Stoichiometric flow rates of anode (s = 2) and cathode (s = 9.5 for O_2 and s = 2 for air) reactants were used at current densities > 0.2 A cm^{-2} and constant flows (corresponding to 0.2 A cm^{-2} flows) at < 0.2 A cm^{-2}. Reactant humidification was achieved by water-bubblers, the temperatures of which were calibrated to yield the desired relative humidity (RH) values. Humidity and cell pressure were measured at the inlet for both electrodes. Cell resistances as a function of current density (i.e., the sum of the proton-conduction resistance in the membrane and the various electronic resistances, bulk and contact resistances) were determined using an AC perturbation of 1 kHz at three different current densities (25, 50 and 100 mA cm^{-2}) and also using a current interrupt method. For each data point, the cell voltage was stabilized for 4 min where the current was measured. Multiple-path serpentine flow-fields (two and three parallel

channels for the anode and cathode, respectively) machined into sealed graphite blocks were used for testing.

The MEAs were conditioned by application of a constant current density of 500 mA cm^{-2} under H_2/Air at 50 kPa gauge, 100% RH and 80 °C. The cell voltage was monitored until a stable value was observed. The conditioning step lasted 2 h unless specified otherwise. Afterwards the cathode catalyst layer was exposed to a series of cathode starvation steps (see below) followed by 2 h current hold at 500 mA cm^{-2} until a stable voltage was observed. After the starvation steps the MEA was ready for testing by a series of H_2/O_2 polarisation curves for MA quantification at different stages of the protocol (50 kPa_{gauge}, 100% RH and 80 °C). The polarisation curves were recorded from low (i.e. 0.05 Acm^{-2}) to high current (i.e. 2 A cm^{-2}) ascending direction and backwards, descending direction. The lower current density limit was determined by maintaining the stoichiometry, at even lower currents there would be a risk of working under over-stoichiometric conditions with the used setup. The current density was maintained for 3 min at each step. The MA value was obtained from the ascending polarisation curve at 0.9 V by extrapolation, after correction for the measured H_2 crossover and cell ohmic resistance. H_2 crossover current densities were measured using the procedure described by Kocha et al. [32]: The hydrogen that permeates through the membrane to the cathode is oxidized by the application of a voltage (typically 250–300 mV are sufficient, and the latest above 400 mV one is in the mass transport limit [19]) and the resulting current measured. Therefore the cell was operated under H_2/N_2 and the gas crossover measurements were done for each operating condition (temperature, H_2-partial pressure). The catalyst activities were evaluated on the basis of H_2 crossover corrected current densities, i_{eff} (i.e., $i_{eff} = i + i_x$, with i_x being on the order of 2–5 A cm^{-2}).

ECSA was measured with the CO stripping method using the cell in half cell mode where the anode electrode acts as a pseudo RE. The cathode voltage was controlled at 0.125 V at 80 °C, 100% RH and 50 kPa_{gauge} whilst purging with 1% CO in N_2 at 300 ml min^{-1} for 15 min, followed by purging with N_2 at the same flow rate for 2 h to ensure that CO is removed from the bubblers and catalyst layer pores. The adsorbed CO is oxidized electrochemically by scanning the cathode voltage from 0.125 V to 0.85 V and back to 0.05 V, at 20 mV s^{-1} for three cycles. The area under the CO oxidation peak is integrated by subtracting the third from the first scan and using a 420 µC cm^{-2} constant for a CO monolayer on Pt [15,28].

The cathode catalyst was tested for durability by LSV under H_2/N_2 and between 0.60 and 0.925 V (LSV1) or between 0.60 and 1.0 V vs. RHE (LSV2) at 50 mV s^{-1}. The catalyst stability was also measured following the current US-DOE catalyst durability protocol as described in table P.1 in Ref. [33]. In this case the voltage was held at 0.60 and 0.925 V for 3 s each. The rise time in between the voltage window of (0.60–0.925) V was controlled with a LSV step at a scan rate of 700 mV s^{-1}. This leads to a rise time of 0.46 s and meets the conditions specified in table P.1. reference [33]. In practical terms, the protocol used in this work is more a triangular wave although it is labelled as SQW for simplicity. The durability protocol was applied for a total of 30,000 cycles, at 80 °C, 100% RH and ambient pressure at the cell outlet. The ECSA was measured via CO stripping at the beginning of the test, after 5000 cycles and at the end of the test. The catalyst MA was monitored at the beginning of life and every 5000 cycles until the end of the test and using a cathode starvation step before running the H_2/O_2 polarisation curve, as specified in the US-DOE tech team fuel cell polarisation protocol, table P.6, steps R1 and R2 (reduction) [33]. The cathode starvation step (purging of cathode compartment with pure nitrogen) reduces the cathode voltage to below 0.1 V and it is intended to provide an electrochemical cleaning step for the cathode catalyst before measuring its activity under H_2/O_2 [33].

2.6. Floating electrode technique

For detailed information about the setup see Ref. [30]. To prepare the hydrophobic floating electrodes, polycarbonate membranes (Sterlitech, PCTF0447100), a sputter machine (Emitech K575X), Teflon AF 2400 powder from DuPont DeNemour, Fluorinert FC-40 liquid from Sigma Aldrich and a vacuum oven were used. The glass cell used was equivalent to the RDE cell but included the electrode holder, constructed from Teflon and Kel-F while the contacts were Au wires. The electrolyte was 1 M $HClO_4$ diluted from Suprapur perchloric acid (Merck) to avoid high ohmic potential drops. The measurement setup consisted of an Autolab potentiostat, a thermostat to keep the cell at 25 °C and a gas supply with N_2, O_2 and H_2. The RE was a RHE and the CE a Pt mesh. The floating WE was prepared as described below, employing a Cole Parmer (KH-02920-00) filtration holder with side arm, a Cole-Parmer (EW-02915-28) 0.2 µm air filter and Whatman (1825150) filter paper.

All Teflon parts and the glassware were pre-cleaned six times by rinsing with ultrapure water, kept for at least 8 h in acidified $KMnO_4$ solution and rinsed again six times. After 1 h in a dilute Caro's acid, all parts were boiled in water and again rinsed six times.

A stock ink solution was produced, consisting of 5 mg Pt/C catalyst, 3 ml solvent (75% Isopropanol, 25% water) and 27 µl Nafion (11.9 wt %) and sonicated for 5 min. A diluted ink was prepared by mixing 4 ml

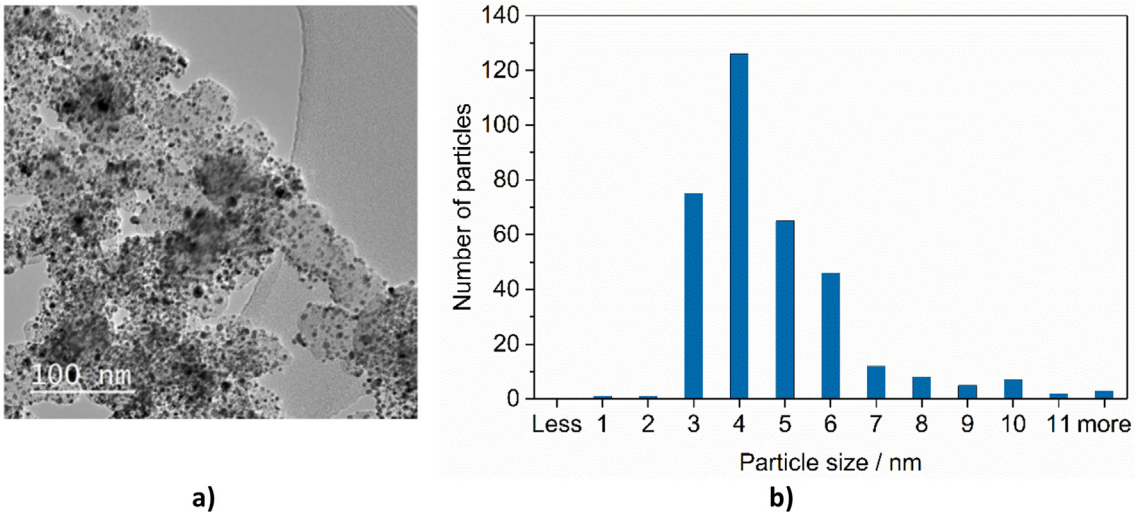

Fig. 1. TEM (a) and particle size distribution (b) for Pt/C catalyst. The mean particle size is 4.1 ± 1.6 nm (for 351 particles analyzed).

solvent with 4.71 µl stock ink with the ultrasound horn, again for 5 min.

The membranes were covered by a 100 nm gold layer using the sputter machine, washed using a Soxhlet extractor for 8 h with isopropanol and afterwards for another 8 h with water. To obtain floating membranes, the back was hydrophobized by depositing 7.5 µl of a 0.25% Teflon AF 2400 in FC 40 solution with a nylon brush. These membranes were dried in a vacuum oven at 100 °C for at least 8 h.

200-450 µl of the diluted ink were transferred onto the membrane with the aid of the filtration setup. The application of suction causes a uniform catalyst coating over the membrane, but also catalyst losses. Therefore, the deposited mass needs to be calculated from ECSA values and the known mass specific surface area of the catalyst.

The electrolyte was purged with nitrogen for 30 min prior to experiments. First 25 cycles (0.05 V–1 V, 100 mV s^{-1}) were carried out under nitrogen atmosphere. After 30 s of hydrogen overflow (i.e. gas flow over the volume above the electrolyte), two voltammetric cycles were measured between −0.1 V and 1 V with 50 mV s^{-1}. Thereafter, 30 s of oxygen overflow was followed by two voltammetric cycles between 1 V and 0 V with 50 mV s^{-1}. Between hydrogen and oxygen flow, the cell was purged with nitrogen. The entire procedure was repeated until the CVs in hydrogen and oxygen were stable. For the ORR performance measurement a CV with two cycles from 1 V to 0 V with 10 mV s^{-1} after at least 30 s oxygen overflow was recorded. A slower scan rate can be used compared to the RDE as there is no convection of possible solution based contaminants to the electrode surface. After the activity measurements, a CV under nitrogen for the ECSA (0.1 V-1 V, 100 mV s^{-1}), a CV under nitrogen under the same conditions as the ORR scan for capacitive background current correction, and an impedance scan for iR correction were performed for similar analysis as in the RDE protocol. The stability testing was similar to that in the RDE measurements, 10,000 cycles between 0.6 and 0.925 V in inert gas atmosphere.

3. Results

3.1. Physical characterization of the catalysts

The characterization data for the Pt/C benchmark reference catalyst (50.4% Pt) are shown in Fig. 1. There is remarkably good agreement between the surface area determined from gas phase adsorption/desorption of CO of 55 m^2 $g_{Pt}{}^{-1}$ and the ECSA determined in the MEA of 55.02 ± 1.15 m^2 $g_{Pt}{}^{-1}$ (5 measurements).

3.2. RDE testing before establishing the protocol

Despite recent publications [17,19–21,24–26,28,29,34], it was considered important to re-evaluate several experimental parameters to establish a testing protocol in order to obtain comparable results between the different laboratories, providing values for ECSA, SA and MA that can be correlated to those obtained in MEA measurements. Those results then should also serve to validate the powerful, but so far rarely used FET technique.

3.2.1. Effect of the catalyst loading on the ORR activity

For obtaining a thin catalyst film on the GC electrode and thus avoiding a possibly increased mass-transport resistance one must adjust the Pt loading. For a 10–50 wt% Pt/C catalyst, a loading of 7–30 μg_{Pt} cm^{-2} has been recommended [26]. In this work loadings of 10, 20 and 30 μg_{Pt} cm^{-2} were investigated. With the lowest loading the diffusion limited ORR current was less than expected from the geometric electrode area, as there was not enough material to cover the entire electrode (Figure S1). Measurements with both 20 and 30 μg_{Pt} cm^{-2} loadings showed typical LSV curves, with the latter reaching a higher (geometric) current density at 0.9 V, but a lower MA. Therefore, the loading of 20 μg_{Pt} cm^{-2} was selected as optimal. For catalysts with different metal/carbon ratio or also for differently active catalysts the optimum loading required to obtain a complete coverage of the electrode and to maintain the thin film condition must be reevaluated. Also it is preferable to evaluate the activity not too close to the diffusion limiting current, as otherwise additional errors are introduced; this condition is better fulfilled for lower loadings.

3.2.2. Effect of the catalyst layer quality

In all three laboratories, efforts were undertaken to optimize the coating conditions. The obtained layer quality can differ significantly despite the standardization of the ink formulation, the preparation and the loading of the catalyst. Spin coating of the ink and static oven drying are equally regarded as valid options for layer preparation, depending on the specific catalyst-support combination and the resulting ink properties. In some cases, even spin coating led to the formation of “coffee rings”, a thicker edge of the layer, and the static oven drying in some cases also produced less uniform layers. Even for catalyst layers prepared by spin-coating under exactly the same conditions and by the same operator showing very similar ECSA values of 59 and 61 m^2g^{-1}, ORR LSVs and the resulting MA at 0.9 V showed larger variations (0.17 A mg^{-1} and 0.22 A mg^{-1}, Figure S2). This emphasizes the

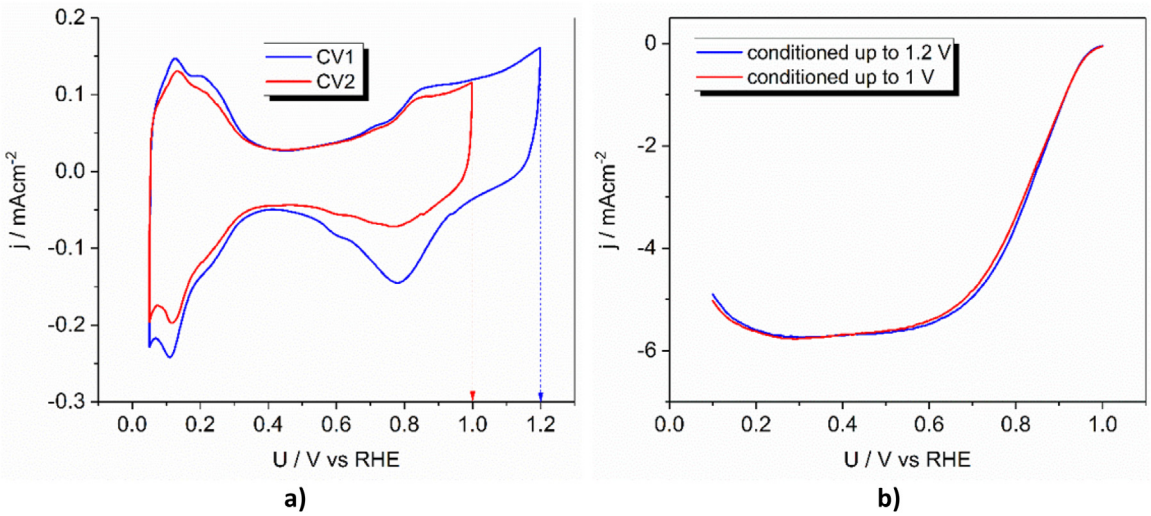

Fig. 2. a) CV for ECSA determination and b) LSV for ORR of a Pt/C reference catalyst conditioned at 1 V (red lines) and 1.2 V (blue lines). Scan rate: 20 mVs^{-1}. (For interpretation of the references to colour in this figure legend, the reader is referred to the Web version of this article.)

essential role of the layer quality. It is therefore important to evaluate the quality of the layers deposited both by a preliminary optical/microscopic screening and by repeating the measurements.

3.2.3. Effect of conditioning upper potential

Catalyst layers are usually preconditioned by cycling in inert gas atmosphere before measuring ECSA and MA in order to remove impurities, ensure full wetting of the catalyst layer and to activate partially passivated catalyst surfaces [24,25]. In Fig. 2a, the stable cycle used for ECSA determination (0.05–1 or 1.2 V in 0.1 M $HClO_4$) for Pt/C conditioned up to 1 V vs. RHE is compared with that conditioned up to 1.2 V. Higher initial Pt oxidation currents together with a higher ECSA value of 70 $m^2 g^{-1}$ compared to 58 $m^2 g^{-1}$ are observed for the electrode preconditioned up to 1.2 V (the larger PtO reduction peak is caused by the stronger Pt oxidation when cycling to 1.2 V). However, the lower ECSA value is much closer to the MEA results and gas phase analysis (cf. 3.1). The higher value after conditioning up to 1.2 V is an indication of Pt surface roughening or Pt dissolution/redeposition induced by the elevated potential. Only slight effects are visible in the LSV curve for ORR activity, which are in excellent agreement (cf. Fig. 2b). Thus, the upper potential was limited to 1 V to minimise surface modifications. Lower upper conditioning potential values are also preferred for alloy catalysts that might leach the less noble metal at elevated potentials.

3.2.4. Effect of CV scan rate on ECSA

Scan rates of 100 and 20 mV s^{-1} were assessed for the ECSA evaluation (Figure S3). The upper potential limit of the UPD region is easily determined. The lower potential limit related to HER onset cannot be clearly distinguished at 100 mV s^{-1} but is clearly visible at 20 mV s^{-1} (cf. inset, Figure S3). Therefore, this scan rate was selected.

3.2.5. Effect of LSV scan rate on ORR evaluation

In literature, there was a strong argument for a scan rate of 20 mV s^{-1} for ORR LSV [24,29]. Nevertheless, 5 mV s^{-1} is often preferred, as there is then no need for a background correction. There is a risk at higher scan rates to apply a too large correction by simple subtraction of the background current measured under Ar. Therefore both scan rates were evaluated and the results validated by the MEA data.

Reduction in scan rate from 20 mV s^{-1} to 5 mV s^{-1} shifts the LSV curve to lower potentials, resulting in lower activity, in agreement with literature (Figure S4a) [24,29]. Background correction at 20 mV s^{-1} leads to a larger value for the MA (Figure S4b). iR correction was applied for all data. Hence, the scan rate of 20 mV s^{-1} was used for further measurements as a good compromise between risk of contamination and of capacitance overcorrection.

3.2.6. Effect of $HClO_4$ purity on the MA and degradation behavior

In a sub-study on electrolyte cleanliness, $HClO_4$ of two different purities was used for preparing 0.1 M $HClO_4$, less pure TRACE select (Fluka) and high purity Ultrex II Ultrapure Reagent (JT Baker). For the higher purity electrolyte, a 30% larger MA was obtained (0.22 A mg^{-1} instead of 0.17 A mg^{-1}). Furthermore, during repeated cycling in O_2 saturated lower purity $HClO_4$ (100 mV s^{-1}, 0.6–0.925 V), interrupted for occasional ORR activity measurements (cf. 3.2.7), the measured ORR currents decreased rapidly. This was not caused by degradation but by impurity adsorption. Reapplying the conditioning procedure followed by ORR measurement led to almost full activity recovery (Fig. 3a). In an ultrapure electrolyte, the changes during repeated cycling were less, and reconditioning had only a minor influence on the ORR LSVs (Fig. 3b). Hence, to minimise surface contamination and reach higher MA, the use of the highest possible acid purity is imperative, in line with literature reports [27].

3.2.7. Effect of different degradation protocols

A common method to investigate catalyst stability is to cycle the potential between 0.6 and 1 V vs. RHE at 100 mV s^{-1} for 10,000 cycles in oxygen saturated solutions [35]. In advanced fuel cell systems, electronic measures are undertaken to assure that the cathode is not exposed to potentials as high as 1 V. Therefore, in a recent revision of the DOE testing protocols for MEAs, an upper potential limit of 0.95 V is used [33]. In this work a value of 0.925 V was considered as appropriate. In general, a protocol must be harsh enough to produce clear changes in activity and ECSA of the catalysts under investigation, and capable of discriminating between catalysts with different stability.

Three different degradation protocols were investigated: Cycling in an

1. O_2 saturated 0.1 M $HClO_4$ solution between 0.6 and 0.925 V for 10,000 cycles at 100 mV s^{-1}
2. O_2 saturated 0.1 M $HClO_4$ solution between 0.2 and 0.925 V for 10,000 cycles at 500 mV s^{-1}

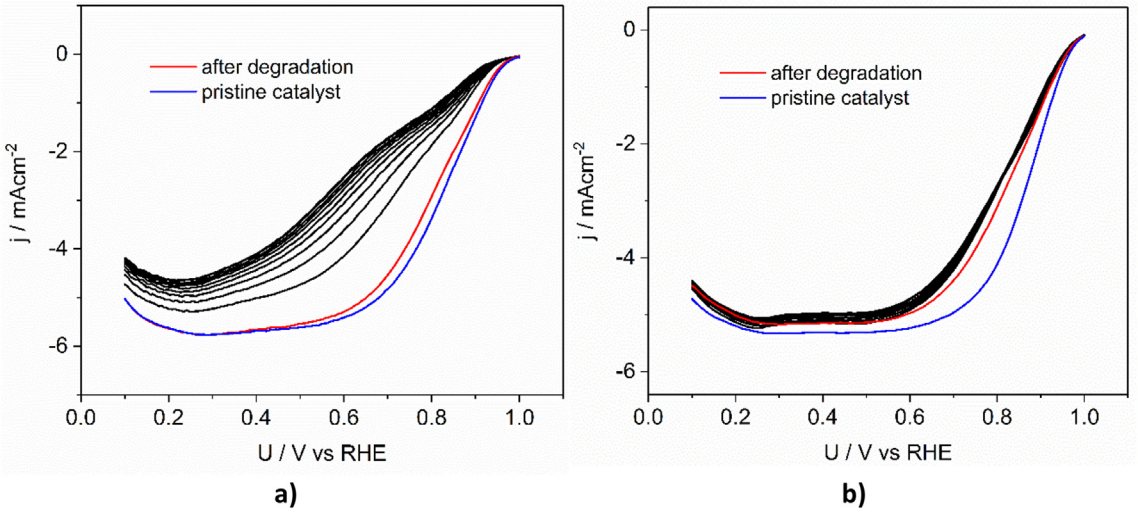

Fig. 3. a) LSV scans for ORR (20 mV s^{-1}, 0.05–1 V) carried out after each 1000th cycle of an accelerated degradation test of a Pt/C reference catalyst in normal purity $HClO_4$ (cycling at 100 mV s^{-1} from 0.6 to 0.925 V vs. RHE in O_2 saturated 0.1 M Fluka TRACEselect $HClO_4$) and b) in ultrahigh purity $HClO_4$ (cycling at 500 mV s^{-1} from 0.2 to 0.925 V vs. RHE in oxygen saturated 0.1M Ultrex II Ultrapure Reagent $HClO_4$). Pristine catalyst (blue lines), aged and reconditioned catalyst (red lines) and scans measured in between the degradation cycles without reconditioning (black lines). (For interpretation of the references to colour in this figure legend, the reader is referred to the Web version of this article.)

3. N_2 saturated 0.1 M $HClO_4$ solution between 0.6 and 0.925 V for 10,000 cycles at 100 mV s^{-1}.

In all three cases active iR compensation was applied during the measurements, as especially the currents in oxygen environment are much larger compared to inert gas and thus could cause potential deviations.

In each case, the full ORR activity measurement procedure (2.4.1–2.4.3) was carried out before and after degradation test. iR corrected CVs under inert gas and LSVs in oxygen corrected for both iR and background (Fig. 4) led to ECSA and MA loss as given in Table 1.

The first protocol led to some MA loss, but the ECSA remained the same. It is known that Pt dissolution as one contributor to catalyst degradation mainly occurs during Pt oxide reduction [36,37]. It was speculated that with the reduced upper potential limit in the presence of oxygen the lower potential was not low enough to fully reduce the surface (hydr)oxide to release significant amounts of Pt into solution. An independent experimental validation of this hypothesis was not in the scope of this work. Therefore, in one set of experiments measurements were carried out under inert gas with the aim of facilitating oxide reduction, and in a second in oxygen with reduced lower potential limit and the scan rate increased to 500 mV s^{-1}. These protocols were able to discriminate between different catalysts, as variations in both ECSA and MA were detected. Due to the more common use of nitrogen saturated media [15,29], protocol 3 was chosen for the final stability testing procedure.

Table 1
Effects of the degradation protocol on the ECSA and mass activity of the reference Pt/C catalyst.

Degradation protocol	ECSA variation	MA loss
0.6–0.925 V (oxygen)	None	20%
0.2–0.925 V (oxygen)	20%	41%
0.6–0.925 V (nitrogen)	20%	23%

3.3. RDE testing after establishing the protocol

Using the established RDE protocol requires also monitoring all the equipment used to detect possible impact. REs used were RHE at Lab1 and 2 and MMS at Lab3. As a CE at Lab1 and 2 either Pt wire or graphite rod were used whereas at Lab3 a Pt mesh wrapped on Pt wire was used. Also different suppliers of the $HClO_4$ were used. Ar was used as an inert gas at Lab2 and N_2 at Lab1 and Lab3. Experiments were carried out at 25 °C at Lab2, at 20 °C at Lab1 and between 22 and 25 °C at Lab3.

The most significant difference was related to the drying procedure after ink application where depending on the available equipment rotation at 700 rpm with (Lab1) or without (Lab2) a lamp (60 W tungsten bulb) or drying in the oven at 60 °C (Lab3) was applied. Although this difference might influence the quality of the obtained catalyst layer and thus activity and stability of the catalysts, the values obtained by the different labs are comparable. Between Lab2 (ECSA = 59 m^2 g_{Pt}^{-1} and MA = 0.24 A mg_{Pt}^{-1}) and Lab1 (ECSA = 61 m^2 g_{Pt}^{-1} and MA = 0.22 A mg_{Pt}^{-1}), the agreement was excellent, while at Lab3 (ECSA = 67.7 m^2 g_{Pt}^{-1} and MA = 0.31 A mg_{Pt}^{-1}), somewhat larger activities and ECSA values were obtained.

3.4. Characterization with the floating electrode technique

Using the FET [30] with a scan rate of 10 mV s^{-1} in 1 M $HClO_4$ led to the voltammograms in Fig. 5. The maximum ORR current densities

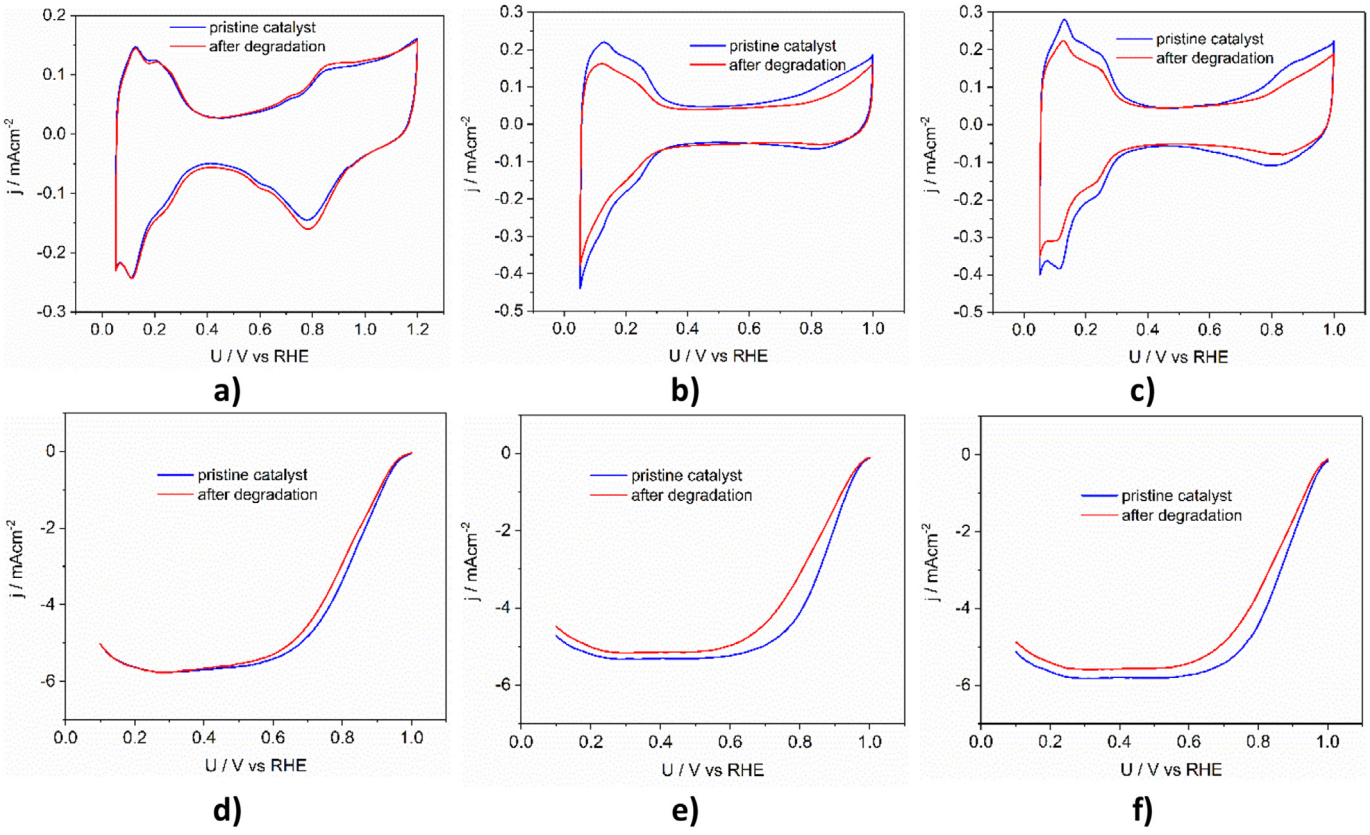

Fig. 4. ECSA (a, b, c) and ORR (d, e, f) of a Pt/C reference catalyst subjected to degradation cycling at 100 mV s^{-1} from 0.6 to 0.925 V vs. RHE in oxygen saturated 0.1 M $HClO_4$ (a, d), at 500 mV s^{-1} from 0.2 to 0.925 V vs. RHE in oxygen saturated 0.1 M $HClO_4$ (b, e) and at 100 mV s^{-1} from 0.6 to 0.925 V vs. RHE in nitrogen saturated 0.1 M $HClO_4$ (c, f). Pristine catalyst (blue lines) and degraded and reconditioned catalyst (red lines). (For interpretation of the references to colour in this figure legend, the reader is referred to the Web version of this article.)

are almost two orders of magnitude higher than possible with RDE, so that the current values at 0.9 V (after iR and background correction) can be used without mass transport correction. In addition, MA could be determined at 0.65 V, which is more representative of actual PEMFC operation conditions. The values for MA at 0.9 V are slightly higher than those obtained by RDE (cf. Table 2).

The application of the same stability protocol as in RDE (cf. 3.2.7 and Fig. 5) led to an ECSA decrease of 20%, in good agreement with RDE and MEA results. The ORR MA decreased by 26% at 0.9 V, and 16% at 0.65 V (Table 2).

Table 2
Results from catalyst testing with the floating electrode technique. For our Pt/C (Pt metal area of 55 $m^2 g^{-1}$, cf. 3.1), a catalyst surface area of 0.103 cm^2 corresponds to a loading of 5.96 µg cm^{-2}. The values between brackets show the percentage decay in surface area and MA (normalized to the original Pt loading) after durability test.

Catalyst	ECSA cm^2	MA @ 0.9 V A mg_{Pt}^{-1}	MA @ 0.65 V A mg_{Pt}^{-1}
Pt/C	0.103	0.39	39
Pt/C aged	0.084 (−19%)	0.29 (−26%)	33 (−16%)

3.5. MEA testing

The catalyst MA was determined under H_2/O_2 as described in section 2.5 (cf. Fig. 6). The excellent linearity in the semi-logarithmic plot especially at lower mass activities (dotted lines) clearly justifies the approach.

The difference between ascending and descending polarisation curves was expected. The MA is higher in the descending direction for most current densities, which means from low to high voltage and usually attributed to less oxide being present on the Pt surface. The same observations have been reported with RDE measurements. The measured hydrogen crossover current is 2.6 mA cm^{-2} and the MA quoted is corrected accordingly (cf. section 2.5). The HOR currents represent less than 10% of the total current; the correction is therefore minor. Studies in aqueous solutions indicated that above 0.8 V the formation of OH_{ad} can cause the HOR current to drop below the limiting current value [29,38], but the deviations reported at 0.9 V are small. In addition, the loadings are much smaller compared to an MEA, therefore a partial oxide coverage will have a much larger impact compared to an MEA, where still enough bare Pt surface is available for HOR at 0.9 V. In MEA it was shown that at least up to 0.8 V the HOR current does not deviate from the limiting current [39], and that the impact of HOR crossover correction at 0.9 V is typically small [40]. Of course, this will depend on the catalyst loading and the membrane; the lower the loading and the larger the hydrogen permeability the larger the chance of incomplete HOR at 0.9 V. In our work, with a high loading and low membrane permeability, the correction with the established procedure [32] is expected to give reliable data: Even if our value for the HOR current would represent a small overestimate, this would have minor impact on the determined MA: At 0.9 V, MA amounts to 0.21 A mg_{Pt}^{-1}. Under these conditions the MA was dependent on the Pt loading and increased with lower loadings. Also, caution needs to be taken when comparing catalysts at different Pt wt% loading as the volumetric roughness factor will be different.

Three different protocols were evaluated for durability testing of the Pt/C catalyst in MEAs (cf. 2.5), resulting in different MA decay (Fig. 7).

The LSV2 protocol with the higher anodic limit is significantly more aggressive than LSV1. The catalyst surface area decreased by 60% and the loss of MA is 57% when the catalyst is cycled up to 1.0 V (cf. Table 3). The use of the SQW protocol led to a faster decay in catalyst surface area compared to LSV1. Similar observations have been reported by Ohma et al. [41] and it is hypothesized that platinum can be easily dissolved at the higher electrode potential if the potential change is fast enough. This will be the case in the SQW protocol used in this work, with a response time < 0.5 s between the voltage limits, and not in the LSV1 protocol where the constant built up of the oxide layer will not allow the exposure of a relatively clean platinum surface to the anodic limit and hence prevent the mechanism that leads to platinum dissolution.

This fast oxidation and reduction of the oxide layer is likely to be the cause that leads to a faster decay in catalyst surface area. Protocol LSV1 was not as aggressive as the other two over the full 30,000 cycles but was sufficient to show clear differences between catalyst formulations. In addition, the upper voltage limit is closer to (but higher than) the value expected to be realised in the automotive fuel cell hardware. Therefore, this protocol was adopted for screening cathode catalyst cyclic stability.

After applying durability protocol LSV1, the ECSA of the Pt/C catalyst decreased from initially 56 to 40 $m^2 g_{Pt}^{-1}$ (29% loss) whereas MA decreased from 0.22 to 0.14 A mg_{Pt}^{-1} (36% loss). The decrease in MA (cf. Table 3) when using LSV1 and SQW protocols is not as pronounced as the decay in surface area. This result was unexpected and it is likely that the cathode reduction step applied in the MA activity is higher than the theoretically expected value for the measured surface area at EOL.

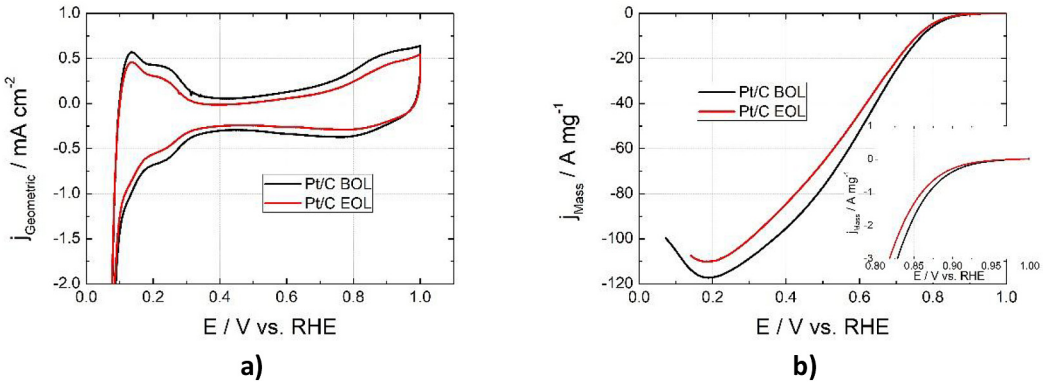

Fig. 5. Floating electrode technique. a) Cyclic voltammograms in nitrogen atmosphere for ECSA determination (0.075–1 V at 100 mV s^{-1} in nitrogen saturated 1 M $HClO_4$). From the determined surface area and the known specific surface area of the catalyst (cf. 3.1), the beginning of life (BOL) mass loading of the electrode can be calculated. b) LSVs for ORR (0–1 V at 10 mV s^{-1} in 1 M $HClO_4$ with the gas space above the electrolyte under O_2) before (black curves) and after (red curves) durability testing at 100 mV s^{-1} from 0.6 to 0.925 V vs. RHE. Inset: magnified view of the high potential region. (For interpretation of the references to colour in this figure legend, the reader is referred to the Web version of this article.)

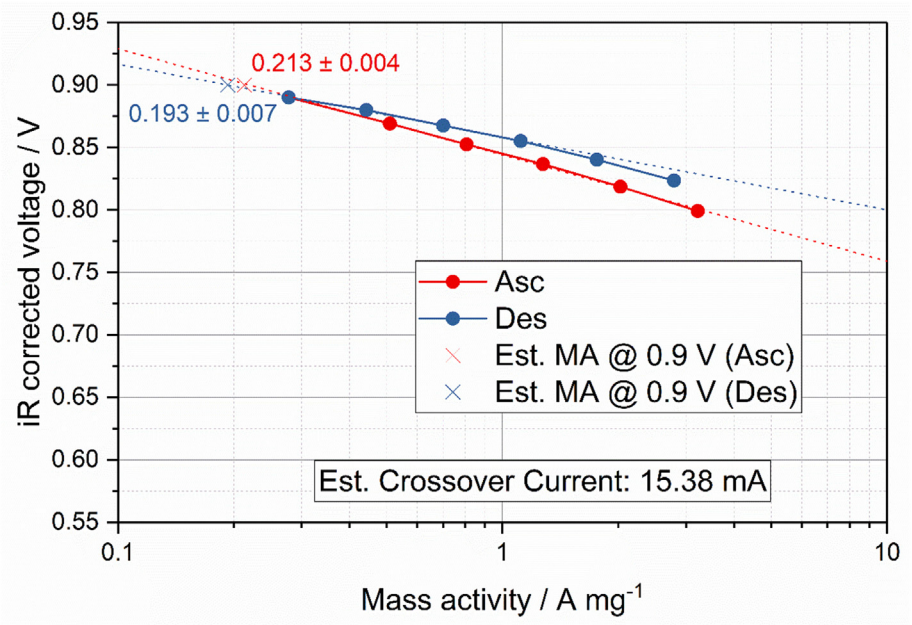

Fig. 6. Mass activity plot for Pt/C catalyst measured in ascending (Asc) and descending (Des) direction. Inlet pressure: 50 kPa, 100% RH @ 80 °C, 6 cm^2 cell. The hydrogen crossover current was measured at 250–300 mV and corresponds to a current density of 2.6 mA cm^{-2}. Loading: 0.20 mg_{Pt} cm^{-2} Pt/C. Dotted lines: linear fits in semi-logarithmic plot of first 5, respectively 4 data points.

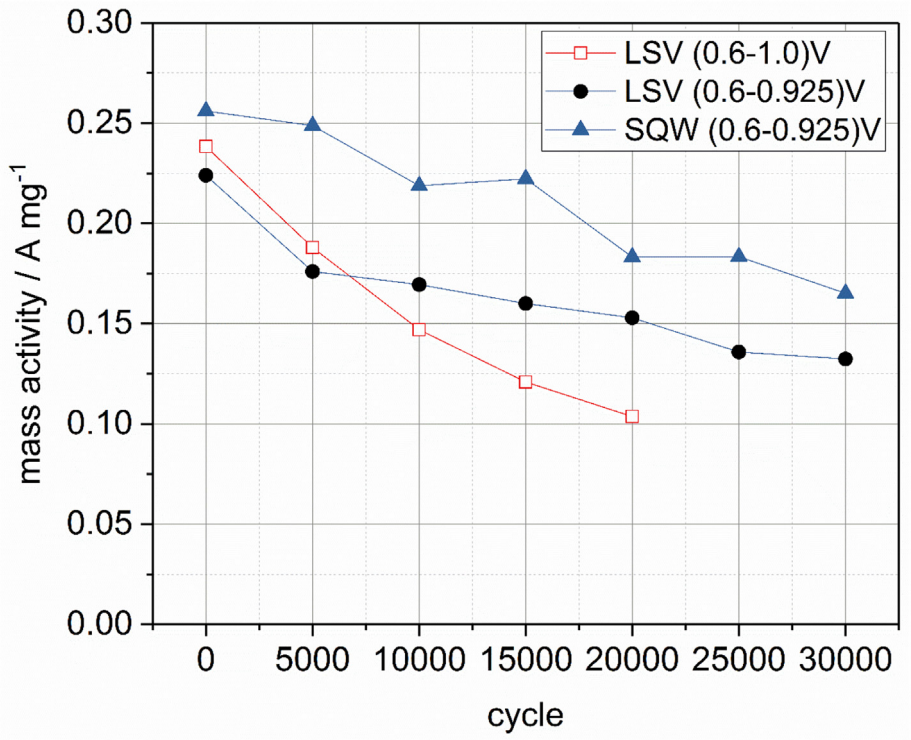

Fig. 7. Mass activity decay for Pt/C benchmark catalyst under three different protocols (cf. Section 2.5).

4. Discussion

RDE is a quick and inexpensive testing method for newly developed catalysts, but very sensitive to the layer quality and the experimental conditions. Therefore, there is often a large scatter of results obtained between different labs but also between different measurements in the same lab, and published results for the same catalysts, even for pure Pt/C, vary substantially [19,42,43]. On the other hand, RDE only provides performance data at extremely low current densities, and the performance at high current densities in an MEA cannot be predicted from those. The first aspect was addressed in this work by establishing an RDE testing protocol with strict instructions for each experimental step of the RDE testing, applied in all labs, the second aspect by carrying out FET measurements working with small catalyst amounts as in RDE but not suffering from small limiting currents.

The RDE results obtained before establishing the full protocol, varying different operation parameters (cf. Section 3), show a large scatter in the ECSA values (58–75 m^2 g_{Pt}^{-1}) and the MA (0.10 and 0.23 A mg_{Pt}^{-1}) (Fig. 8a). Using the established protocol, the values obtained by the different labs are much better comparable (cf. Fig. 8a, large open circles), and the ECSA values from Lab1 and Lab2 (cf. 3.3) are close to the surface area determined by gas phase techniques (cf. 3.1). The only appreciable difference between the labs after establishing the protocol concerned the drying procedure after ink application (cf. section 2.2)

Table 3
Summary of results for the Pt/C benchmark catalyst tested for durability using the three different protocols. The Pt loading on the anode and cathode was 0.10 and 0.20 mg_{Pt} cm^{-2}, respectively. EOL stands for end of life. The values between brackets show the percentage decay in normalized ECSA and MA after durability test.

Protocol	Electrochemical surface Area in MEA (CO) ($m^2 g_{Pt}^{-1}$)		O_2 Mass Act at 0.9 V/ ($A mg_{Pt}^{-1}$)	
	BOL	EOL	BOL	EOL
LSV1, (0.6–0.925) V	56	40 (−29%)	0.22	0.14 (- 36%)
LSV2, (0.6–1.0) V	51	20 (−60%)	0.23	0.10 (−57%)
SQW, (0.6–0.925) V	60	28 (−54%)	0.26	0.16 (−39%)

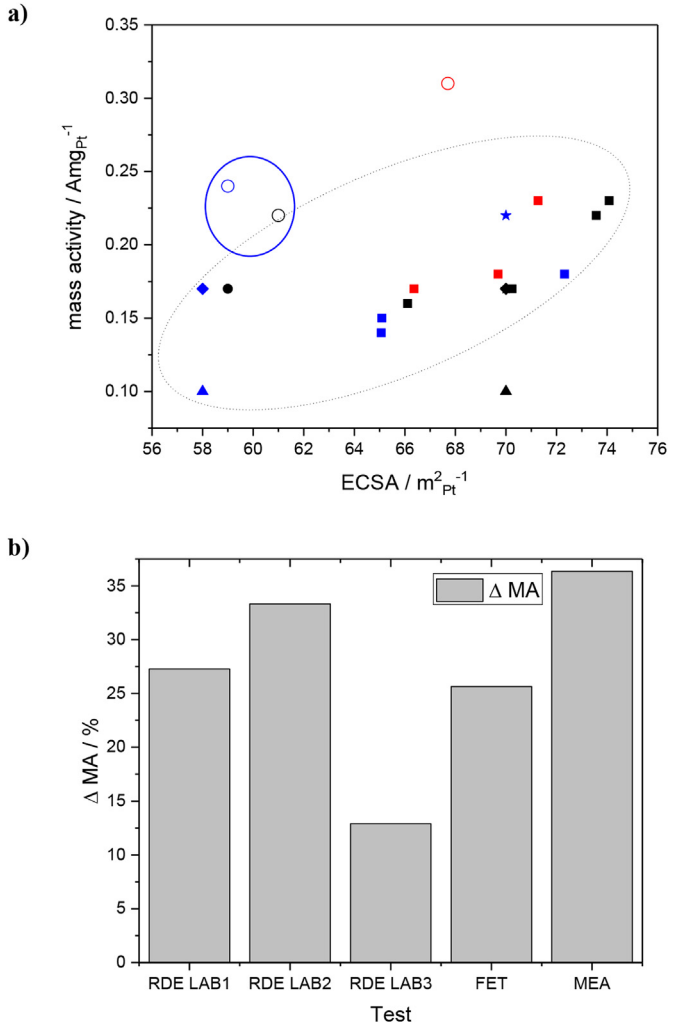

Fig. 8. a) Mass activities and ECSA of the Pt/C catalyst obtained by RDE testing for the different experimental conditions before (small symbols, catalyst loading (squares, cf. 3.2.1), layer quality (circles, cf. 3.2.2), scan rate and conditioning potential range (triangles, cf. 3.2.3–3.2.5) and acid purity (stars, cf. 3.2.6) were varied) and after the final protocol was established (large open circles, 3.3). Black: Lab1, blue: Lab2, red: Lab3. b) Relative decrease in mass activity for Pt/C after the degradation protocols applied with the three different methods (RDE, FET, MEA single cell testing). (For interpretation of the references to colour in this figure legend, the reader is referred to the Web version of this article.)

which caused small deviations at Lab3 (large open red circle). This emphasizes once more the significance of obtaining good quality layers and following the strict protocol for evaluating catalyst performance. This, as well as the best choices for several operating parameters, are in good agreement with newer literature [13,22].

The activities obtained from RDE measurements were further compared to those obtained by FET and MEA testing. For this, one has to be aware of the differences between the methods. In RDE measurements, a correction for mass transport needs to be made to obtain the kinetic current at 0.9 V. Then this value can be compared with the activity obtained by FET at the same potential without mass transport correction. Further, the MEA is tested in a pseudo-steady state, holding the potential for 4 min at each point to allow for some equilibration of the Pt/Pt-oxide surface, whereas the RDE and FET are measured dynamically. In addition, there are differences in the catalyst layer structure, the operation temperature and the electrolyte. Therefore a full quantitative agreement cannot be expected; more important is that actual trends between different catalysts and with respect to the ageing behavior are correctly represented. Mass activities obtained by FET (0.39 A mg_{Pt}^{-1}) and in MEAs testing (0.21–0.26 A mg_{Pt}^{-1}) are still in reasonable agreement with those ones obtained in RDE measurements, given the different operation conditions. It is also important to highlight that the oxide coverage on the catalyst surface at 0.9 V will be different for the three methods used in this work contributing to MA differences. This will be subject of further work and will be addressed with the use of Pt and platinum alloy catalysts.

In MEAs, the performance also at high current densities and thus at much lower cell voltages (like 0.65 V) than in RDE is of interest. In these conditions, mass transport phenomena inside the catalyst layer are very important, and the actual surface area of the catalyst, the particle size and number density play a huge role, factors that are irrelevant at 0.9 V. This is especially true for catalysts with ECSA below 60 m^2 g_{Pt}^{-1}, as found by JMFC and explained by the mass transport issues in the catalyst layers. Thus catalysts can perform great at 0.9 V in the RDE test, but rather poor at larger current densities during MEA testing. Unlike the RDE, where this behavior cannot be screened, the FET is not mass transport limited at current densities in the more relevant potentials region for FCs, between 0.6 and 0.8 V vs. RHE. During FET electrode preparation, part of the applied catalyst is lost. The amount present on the electrode can be calculated via H_{UPD} measurement or by CO stripping (providing the active catalyst area in m^2). Thereafter both SA and MA can be evaluated over a large potential range, enabling further correlation with MA obtained in MEAs at high current densities. Therefore, this method is a big advancement compared to RDE measurements, providing significantly more information, while still requiring small amounts of catalyst and rather inexpensive equipment. Since the catalyst layer structure and the experimental conditions are not identical, only activity trends are represented correctly.

Newly developed catalysts need to show good stability as well. In this work, three different durability protocols were evaluated for durability testing in 6 cm^2 MEAs (cf. section 3.5). In each successive cycle surface oxidation and reduction cause accelerated catalyst degradation. Different degradation stadiums can be traced by recording polarisation curves and evaluating ECSA at specified intervals. MA at the end of the test can be compared with the one before durability test. Previously, in MEAs, the stability was evaluated by the degradation test between 0.6 and 1.0 V. This potential range was acceptable for the evaluation of Pt/C catalysts degradation but these conditions are too harsh for Pt-alloy catalysts. In the newer FC technology the upper potential is limited to less than 0.95 V. The very harsh conditions of the LSV2 test were also observed in this work (cf. Table 3). The protocols with the 0.925 V upper potential triggers changes in Pt/C but conditions are not too harsh for alloys. However, the LSV1 protocol only caused changes over the first 5000 cycles. A full validation of the procedure requires application to different catalysts and more detailed studies. Nevertheless, the LSV1 protocol appeared to be the best to derive the corresponding RDE protocol from. For actual MEA testing, the SQW protocol might be the better one, causing degradation throughout the entire experimental

duration.

The protocol for the RDE stability test was therefore based on LSV1. Cycling between 0.6 and 0.925 V in N_2 was selected as the method of choice, producing a clear decrease in both ECSA and MA, without being overly harsh. With exception of the results in Lab3, results obtained by RDE, FET and MEA show reasonable agreement for the MA decrease despite the different operation temperature (Fig. 8b).

The results in this work show that indeed RDE testing can provide comparable results from test to test and in between different labs, provided that a strict protocol is followed, and accurate cleanliness is maintained. Also control of the layer quality is necessary. The specific recipe for ink formulation and layer application must be optimized for each different catalyst/support combination. Then, suitable catalysts can be selected for further screening. Ideally, this should involve FET measurements in order to evaluate the high current performance, before catalyst preparation is up-scaled for MEA testing.

5. Conclusions

A Pt/C catalyst was used to develop a detailed RDE testing protocol enabling to correlate activity and stability determined by RDE with values obtained from the FET and MEA testing. This was achieved by studying the influence of a variety of parameters on ECSA and MA, as well as different stability protocols. As result highly reproducible activity values were obtained that were very well comparable between three different labs. When the coating was applied under rotation, the agreement was excellent, while drying of the coating in an oven without rotation led to slightly larger activities. In comparison to RDE, FET allows to test the catalyst performance at much larger ORR reduction currents. While the absolute MA numbers at 0.9 V differed between RDE, FET and MEA, these measurements should provide the correct trend when comparing different catalysts. They do show the right trends regarding material stability, as the relative decrease in MA with optimized degradation protocols are well comparable. Precise RDE measurements are therefore an excellent tool for preliminary screening of fuel cell catalyst materials.

Acknowledgements

The project leading to this application has received funding from the Fuel Cells and Hydrogen 2 Joint Undertaking under grant agreement No 700127. This Joint Undertaking receives support from the European Union's Horizon 2020 research and innovation programme and Hydrogen Europe and N.ERGHY. TUB acknowledges Annette Wittebrock for her help in the laboratory. TUM acknowledges H. El-Sayed for helpful discussions.

Appendix A. Supplementary data

Supplementary data related to this article can be found at http://dx.doi.org/10.1016/j.jpowsour.2018.04.084.

References

[1] L. Ager-Wick Ellingsen, C. Roxanne Hung, G. Majeau-Bettez, B. Singh, Z. Chen, M. Stanley Whittingham, A. Hammer Strømman, Nat. Nanotechnol. 11 (2016) 1039–1051.
[2] F.T. Wagner, B. Lakshmanan, M.F. Mathias, J. Phys. Chem. Lett. 1 (2010) 2204–2219.
[3] O. Gröger, H.A. Gasteiger, J.-P. Suchsland, J. Electrochem. Soc. 162 (2015) A2605–A2622.
[4] R. Othman, A.L. Dicks, Z. Zhu, Int. J. Hydrogen Energy 37 (2012) 357–372.
[5] H.A. Abaoud, M. Ghouse, K.V. Lovell, G.N. Al-Motairy, Int. J. Hydrogen Energy 30 (2005) 385–391.
[6] I.E.L. Stephens, A.S. Bondarenko, U. Gronbjerg, J. Rossmeisl, I. Chorkendorff, Energy Environ. Sci. 5 (2012) 6744–6762.
[7] A. Rabis, P. Rodriguez, T.J. Schmidt, ACS Catal. 2 (2012) 864–890.
[8] M.K. Debe, Nature 486 (2012) 43–51.
[9] J. Wu, X.Z. Yuan, J.J. Martin, H. Wang, J. Zhang, J. Shen, S. Wu, W. Merida, J. Power Sources 184 (2008) 104–119.
[10] H. Duan, C. Xu, Electrochim. Acta 152 (2015) 417–424.
[11] M.E. Scofield, H. Liu, S.S. Wong, Chem. Soc. Rev. 44 (2015) 5836–5860.
[12] Z. Chen, D. Higgins, A. Yu, L. Zhang, J. Zhang, Energy Environ. Sci. 4 (2011) 3167–3192.
[13] M. Shao, Q. Chang, J.-P. Dodelet, R. Chenitz, Chem. Rev. 116 (2016) 3594–3657.
[14] A. Morozan, B. Jousselme, S. Palacin, Energy Environ. Sci. 4 (2011) 1238–1254.
[15] K. Shinozaki, J.W. Zack, R.M. Richards, B.S. Pivovar, S.S. Kocha, J. Electrochem. Soc. 162 (2015) F1144–F1158.
[16] N. Wakabayashi, M. Takeichi, M. Itagaki, H. Uchida, M. Watanabe, J. Electroanal. Chem. 574 (2005) 339–346.
[17] H.A. Gasteiger, J.E. Panels, S.G. Yan, J. Power Sources 127 (2004) 162–171.
[18] J. Lilloja, E. Kibena-Põldsepp, M. Merisalu, P. Rauwel, L. Matisen, A. Niilisk, E.S.F. Cardoso, G. Maia, V. Sammelselg, K. Tammeveski, Catalysts 6 (2016) 108–126.
[19] H.A. Gasteiger, S.S. Kocha, B. Sompalli, F.T. Wagner, Appl. Catal., B 56 (2005) 9–35.
[20] U.A. Paulus, T.J. Schmidt, H.A. Gasteiger, R.J. Behm, J. Electroanal. Chem. 495 (2001) 134–145.
[21] T.J. Schmidt, H.A. Gasteiger, G.D. Stäb, P.M. Urban, D.M. Kolb, R.J. Behm, J. Electrochem. Soc. 145 (1998) 2354–2358.
[22] F.A. Viva, G.A. Olah, G.K.S. Prakash, Int. J. Hydrogen Energy 42 (2017) 15054–15063.
[23] J. Qiao, L. Xu, Y. Liu, P. Xu, J. Shi, S. Liu, B. Tian, Electrochim. Acta 96 (2013) 298–305.
[24] Y. Garsany, J. Ge, J. St-Pierre, R. Rocheleau, K.E. Swider-Lyons, J. Electrochem. Soc. 161 (2014) F628–F640.
[25] Y. Garsany, I.L. Singer, K.E. Swider-Lyons, J. Electroanal. Chem. 662 (2011) 396–406.
[26] Y. Garsany, O.A. Baturina, K.E. Swider-Lyons, S.S. Kocha, Anal. Chem. 82 (2010) 6321–6328.
[27] K. Shinozaki, J.W. Zack, S. Pylypenko, B.S. Pivovar, S.S. Kocha, J. Electrochem. Soc. 162 (2015) F1384–F1396.
[28] K.J.J. Mayrhofer, D. Strmcnik, B.B. Blizanac, V. Stamenkovic, M. Arenz, N.M. Markovic, Electrochim. Acta 53 (2008) 3181–3188.
[29] C.M. Pedersen, M. Escudero-Escribano, A. Velázquez-Palenzuela, L.H. Christensen, I. Chorkendorff, I.E.L. Stephens, Electrochim. Acta 179 (2015) 647–657.
[30] C.M. Zalitis, D. Kramer, A.R. Kucernak, Phys. Chem. Chem. Phys. 15 (2013) 4329–4340.
[31] F. Hernández Ramírez, Ph.D. Thesis, Rheinische Friedrich-Wilhelms-Universität Bonn, Bonn, 2006.
[32] S.S. Kocha, Principles of MEA preparation, Handbook of Fuel Cells, John Wiley & Sons, Ltd, 2010.
[33] Fuel Cell Technologies Office Multi-Year Research, Development, and Demonstration Plan Section 3.4 Fuel Cells, Office of Energy Efficiency and Renewable Energy, 2017, https://energy.gov/sites/prod/files/2017/05/f34/fcto_myrdd_fuel_cells.pdf.
[34] S.S. Kocha, K. Shinozaki, J.W. Zack, D.J. Myers, N.N. Kariuki, T. Nowicki, V. Stamenkovic, Y. Kang, D. Li, D. Papageorgopoulos, Electrocatalysis 8 (2017) 366–374.
[35] P. Hernandez-Fernandez, F. Masini, D.N. McCarthy, C.E. Strebel, D. Friebel, D. Deiana, P. Malacrida, A. Nierhoff, A. Bodin, A.M. Wise, J.H. Nielsen, T.W. Hansen, A. Nilsson, I.E.L. Stephens, I. Chorkendorff, Nat. Chem. 6 (2014) 732–738.
[36] P.P. Lopes, D. Strmcnik, D. Tripkovic, J.G. Connell, V. Stamenkovic, N.M. Markovic, ACS Catal. 6 (2016) 2536–2544.
[37] S. Cherevko, G.P. Keeley, S. Geiger, A.R. Zeradjanin, N. Hodnik, N. Kulyk, K.J.J. Mayrhofer, ChemElectroChem 2 (2015) 1471–1478.
[38] Y.-J. Deng, M. Arenz, G.K.H. Wiberg, Electrochem. Commun. 53 (2015) 41–44.
[39] M. Schalenbach, T. Hoefner, P. Paciok, M. Carmo, W. Lueke, D. Stolten, J. Phys. Chem. C 119 (2015) 25145–25155.
[40] S. Kocha Shyam, J. Deliang Yang, S. Yi Jung, AIChE J. 52 (2006) 1916–1925.
[41] A. Ohma, K. Shinohara, A. Iiyama, T. Yoshida, A. Daimaru, ECS Trans. 41 (2011) 775–784.
[42] T. Toda, H. Igarashi, H. Uchida, M. Watanabe, J. Electrochem. Soc. 146 (1999) 3750–3756.
[43] U.A. Paulus, A. Wokaun, G.G. Scherer, T.J. Schmidt, V. Stamenkovic, N.M. Markovic, P.N. Ross, Electrochim. Acta 47 (2002) 3787–3798.